Cavity QED analog of the harmonic-oscillator probability distribution function and quantum collapses

Z. Ficek[1,2] and S. Swain[1]
[1]*Department of Applied Mathematics and Theoretical Physics, The Queen's University of Belfast, Belfast BT7 1NN, Northern Ireland*
[2]*Department of Physics and Centre for Laser Science, The University of Queensland, Brisbane QLD 4072, Australia*
(Received 10 January 2001; published 16 May 2001)

We establish a connection between the simple harmonic oscillator and a two-level atom interacting with resonant, quantized cavity and strong driving fields, which suggests an experiment to measure the harmonic-oscillator's probability distribution function. To achieve this, we calculate the Autler-Townes spectrum by coupling the system to a third level. We find that there are two different regions of the atomic dynamics depending on the ratio of the Rabi frequency Ω_c of the cavity field to that of the Rabi frequency Ω of the driving field. For $\Omega_c<\Omega$ and moderate coupling of the transition to the cavity mode the spectral peaks are composed of multiplets. A quantized dressed-atom approach provides a simple explanation of the spectral features and shows that the oscillations in the spectral components arise from the oscillations of the population distribution in the dressed states. The observation of these features would provide evidence for the quantum nature of the cavity field. The distribution is an analog of the harmonic-oscillator probability distribution function, and should be experimentally observable. For $\Omega_c \geqslant \Omega$ there is no Autler-Townes splitting and the spectrum is composed of a single peak located at the frequency of the probe transition. We show that this effect results from the collapse of the atom to the ground state, which has been predicted by Alsing, Cardimona, and Carmichael [Phys. Rev. A **45**, 1793 (1992)] for a two-level atom in a lossless cavity.

DOI: 10.1103/PhysRevA.63.063815 PACS number(s): 42.50.Ct, 03.65.−w, 32.80.−t

I. INTRODUCTION

With recent successful experiments in the laser cooling and trapping of a single atom within a single mode of a microscopic cavity [1], it is now possible to test theoretical predictions of quantum physics [2] and the cavity quantum electrodynamics (CQED) of the strong interaction of atoms with single quanta of the radiation field. The fundamental model of the atom-field interaction is the Jaynes-Cummings model [3] consisting of an excited two-level atom strongly coupled to a single mode of the radiation field. The model has been extensively studied and many interesting quantum effects have been predicted and observed, among the most well known of which are collapse and revival of the inversion [4], subnatural linewidths [5], fluorescence spectra [6,7], and nonclassical photon statistics [8]. These features result from the presence of a multiple exchange of photons between the radiating atom and the cavity mode and occur when the coupling strengths between the atom and the cavity mode are larger than the damping rates of the system.

The Jaynes-Cummings model has been extended to include spontaneous emission, cavity damping, and external driving fields. Two different configurations of atom driving have been analyzed. In the first case the external field drives the cavity mode [8,9], and in the second case the driving field couples to the atom through an auxiliary field, different than the cavity mode [7,10]. The cases of strong and weak atom-cavity couplings have been considered. In the case of the atom driven through an auxiliary mode and weak atom-cavity coupling the system behaves formally the same as in free space, but with significantly modified spontaneous-emission rates. For instance, the fluorescence spectrum of a strongly driven atom is a triplet, as in free space [11], but with widely differing linewidths. Depending on the detuning of the cavity mode from the atomic resonance, the central or even all three spectral components can be significantly narrowed [12]. For strong atom-cavity coupling, each Mollow triplet component is composed of a multiplet, whose detailed structure depends on the atom-cavity coupling strength, the cavity and spontaneous-emission decay rates, and the photon-number distribution of the cavity field [6,7]. Moreover, in the case of the lossless cavity and exact resonance of the cavity and the driving fields to the atomic transition frequency, the atom can remain in its ground state resulting in the disappearance of the atomic resonance fluorescence [10].

Recently, considerable interest in the study of the Jaynes-Cummings model has been devoted to observing the signatures of the discrete nature of field quanta in the atom-cavity interaction that are sensitive to the presence of single quanta in the cavity mode. The most recent are experiments on the detection of quantum Rabi oscillations [13], Fock states of the radiation field [14], and a quantum phase gate [15]. However, the basic signature of a discrete small number of photons in the cavity mode is the dependence of the energy spectrum of the Jaynes-Cummings model on the number of photons n. The energy spectrum is composed of a single ground $(n=0)$ level, and a ladder of doublets separated by $\hbar\omega_0$. The intradoublet splitting is equal to $\hbar g\sqrt{n}$, where ω_0 is the resonance frequency and g is the atom-cavity coupling constant. The splitting is characterized by $\sqrt{n}$, the signature of a discrete number of photons in the cavity mode. The splitting of the lowest energy doublet $(n=1)$, called the vacuum Rabi splitting, has been observed experimentally [16], and a photon correlation spectroscopy technique involving a weak multichromatic field has been proposed to measure the unequal splitting of the second and third

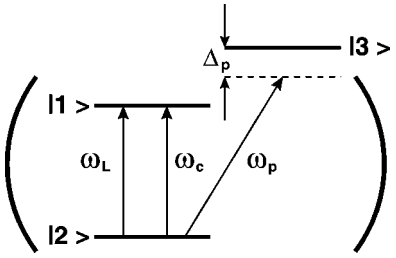

FIG. 1. Schematic diagram of a three-level atom driven by a coherent laser field of the frequency ω_L equal to the atomic transition frequency ω_{12} and coupled to a cavity mode of the frequency $\omega_c=\omega_L$.

excited-state doublets [17]. Since the splittings are unequal, the absorption resonances of the multichromatic field will be proportional to $(\sqrt{n}-\sqrt{n-1})$, where $n=1,2,\ldots$. These resonances vanish in the classical limit of $n\gg 1$.

Another elementary system which is sensitive to the presence of single quanta is a particle confined in a box [18]. This system is qualitatively similar to a harmonic oscillator whose position operator exhibits a discrete spectrum such that the probability of finding the particle at the dimensionless position $\xi=(m\omega/\hbar)^{1/2}x$ inside the box depends on ξ and the number of quanta n. The probability is maximal in the vicinity of the classical turning points of the harmonic-oscillator eigenfunction $\phi_n(\xi)$, i.e., for $\xi_n\sim\pm 2\sqrt{n+\frac{1}{2}}$, or for energies $|\xi_n|\hbar\omega_0$. For $|\xi|>|\xi_n|$ the probability goes rapidly to zero, while for $\xi<|\xi_n|$ the probability is nonzero and oscillates with ξ. The number of oscillations depends on n and reveals the discrete energy spectrum of the system. In the classical limit of a large number of quanta $(n\gg 1)$ the change in the number of oscillation with n is unnoticeable.

The harmonic-oscillator probability distribution is one of the fundamental quantities of quantum mechanics, and is discussed in almost all textbooks on the subject, yet it has never been experimentally verified. In this paper we draw an analogy between this system and that of a strongly driven two-level atom interacting with a quantized cavity mode, which should permit the observation of this probability distribution. We investigate the Autler-Townes spectrum of a three-level atom where one of the transitions is coupled to a single cavity mode and is driven, through an auxiliary mode, by a strong coherent laser field. The cavity and the laser field frequencies are assumed to be equal and resonant with the atomic transition frequency. We find that the spectrum contains the oscillatory signature of the probability distribution function of the harmonic oscillator.

II. THE DRIVEN CAVITY AND THE HARMONIC OSCILLATOR

We first consider a two-level atom with ground state $|2\rangle$ and excited state $|1\rangle$, with transition frequency ω_{12}. The transition $|2\rangle-|1\rangle$ is coupled to a cavity mode and driven through an auxiliary mode by a classical laser field (see Fig. 1). We employ a dressed-state approach in which we quantize both the cavity and driving laser fields. The Hamiltonian of the system is

$$H=H_0+H_{int}, \tag{1}$$

where

$$H_0=\hbar\omega_{12}(a^\dagger a+a_L^\dagger a_L+S_1^+S_1^-) \tag{2}$$

is the unperturbed Hamiltonian, and

$$H_{int}\equiv V+V_L=\hbar g(S_1^+a+a^\dagger S_1^-)+\hbar g_L(S_1^+a_L+a_L^\dagger S_1^-) \tag{3}$$

is the interaction between the atom and the fields, where a and a_L are the annihilation operators of the cavity and laser modes, g and g_L are the atom-cavity and atom-laser coupling constants, respectively, and $S_1^+=|1\rangle\langle 2|$, $S_1^-=|2\rangle\langle 1|$ are the atomic raising and lowering operators of the $|1\rangle-|2\rangle$ transition. In this section we neglect all damping effects.

The eigenstates of H_0 are the product states $|i,N_L,n\rangle=|i\rangle\otimes|N_L\rangle\otimes|n\rangle$, where $|i\rangle$ is an atomic state $(i=1,2)$, N_L is the number of photons in the laser mode, and n is the number of photons in the cavity mode. The states $|i,N_L,n\rangle$ form an infinite ladder of sets of highly degenerate states of energies $\hbar(N_L+n)\omega_{12}$. We first diagonalize the Hamiltonian consisting of the unperturbed Hamiltonian plus the interaction with the laser field, $H_1\equiv H_0+V_L$. This gives rise to the singly dressed states that have the form

$$H_1|N_L\pm,n\rangle=\hbar[(N_L+n)\omega_{12}\pm\Omega]|N_L\pm,n\rangle, \tag{4}$$

where $\Omega=2g\sqrt{\langle N_L\rangle}$, $|N_L\pm,n\rangle\equiv|N_L,\pm\rangle|n\rangle$ and the $|N_L,\pm\rangle$ are the conventional two-level atom dressed states [20]. Finally, including the weak interaction V, we obtain doublet continua $E_{N,d_i,\lambda}$ and eigenstates $|N,d_i,\lambda\rangle$ which satisfy the eigenvalue equation

$$H|N,d_i,\lambda\rangle=E_{N,d_i,\lambda}|N,d_i,\lambda\rangle \quad (i=1,2), \tag{5}$$

where we use the label d_i to indicate dressed states,

$$E_{N,d_i,\lambda}=N\hbar\omega_{12}+(-1)^i\left(\frac{1}{2}\Omega+\lambda g\right), \tag{6}$$

$$|N,d_i,\lambda\rangle=\sum_{n=1}^{\infty}\phi_n\left((-1)^i\frac{\lambda}{\sqrt{2}}\right)|i,N,n\rangle, \tag{7}$$

with

$$\phi_n(x)=(\sqrt{2\pi}2^n n!)^{-1/2}H_n(x)e^{-(1/2)x^2}, \tag{8}$$

where $N=N_L+n$ is the total number of photons in the field modes and λ is an arbitrary real number $(-\infty<\lambda<\infty)$ (cf. [21]).

The functions defined in Eq. (8) are just the energy eigenfunctions of the harmonic oscillator in the coordinate representation, as discussed in almost all textbooks on quantum mechanics. We have thus established an intimate connection between the driven two-level atom in a good cavity and the harmonic oscillator. This connection is further reinforced by noting that the matrix elements of the cavity interaction V in terms of the singly dressed eigenstates of H_1 are

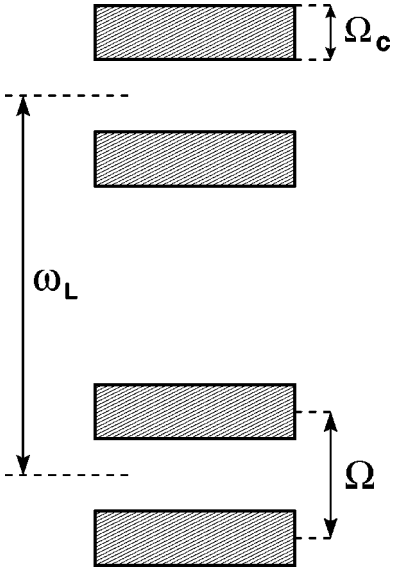

FIG. 2. Energy levels of the system. Each energy manifold is composed of two continua of widths equal to the Rabi frequency Ω_c of the cavity field and separated by the Rabi frequency Ω of the driving field.

$$\langle N_L\pm,n|V|N_L\pm,m\rangle=\pm\frac{1}{2}\hbar g(\sqrt{n+1}\,\delta_{n+1,m}+\sqrt{n}\,\delta_{n-1,m}) \tag{9}$$

where we have assumed negligible interaction between the + and — manifolds, which is true when the laser Rabi frequency exceeds the cavity Rabi frequency. This matrix is identical to that which represents the position operator of the harmonic oscillator in the basis of the energy eigenstates [18]. In fact, it is shown in [22] that the eigenstates of the position operator of the harmonic oscillator in the basis of its energy eigenstates are just the functions (8).

From Eqs. (6) and (7) we can easily predict the energy spectrum of the system. Since λ is an arbitrary real number, analogous to the coordinate of the one-dimensional harmonic oscillator, discrete energy levels of the system *do not* exist. In this case the energy spectrum of the system, shown in Fig. 2, is composed of an infinite ladder of doublet continua with interdoublet separation ω_{12} and intradoublet splitting Ω.

It is our major purpose here to suggest ways of measuring $|\phi_n(x)|^2$, the probability distribution function of the harmonic oscillator [18]. One way of achieving this is to couple the ground state to a third level which may be probed by a second, weak, tunable laser. This is considered in the next section, where we also introduce damping.

III. CAVITY MODIFIED MASTER EQUATION

We now consider a three-level atom with ground state $|2\rangle$ and two excited states $|1\rangle$ and $|3\rangle$. The transition $|2\rangle-|1\rangle$ is coupled to the cavity mode and driven through an auxiliary mode as before, but now the driving field is a classical laser field. The transition $|2\rangle-|3\rangle$, which is not coupled to the cavity mode, is probed by a weak laser field that monitors the cavity effects on the coherently driven transition (see Fig. 1). We assume that the dipole moments of the transitions $\vec{\mu}_{12}$ and $\vec{\mu}_{32}$ are perpendicular to each other so that no correlation exists between the transitions. In the interaction picture, the master equation of the system is

$$\frac{d\rho}{dt}=-\frac{i}{\hbar}[H,\rho]+L_c\rho+L_a\rho, \tag{10}$$

where

$$H=\hbar\Delta_c a^\dagger a+\hbar\Delta_a S_1^+S_1^-+\hbar\Delta_p S_3^+S_3^-+\hbar g(S_1^+a+a^\dagger S_1^-)$$
$$+\frac{\hbar}{2}\Omega(S_1^++S_1^-)+\frac{\hbar}{2}\Omega_p(S_3^++S_3^-) \tag{11}$$

is the Hamiltonian of the probed and driven atom-cavity system in the frame rotating with the laser frequency ω_L,

$$L_c\rho=\frac{1}{2}\kappa(2a\rho a^\dagger-a^\dagger a\rho-\rho a^\dagger a) \tag{12}$$

is the damping operator of the cavity field, and

$$L_a\rho=\frac{1}{2}\Gamma_1(2S_1^-\rho S_1^+-S_1^+S_1^-\rho-\rho S_1^+S_1^-) \tag{13}$$

$$+\frac{1}{2}\Gamma_3(2S_3^-\rho S_3^+-S_3^+S_3^-\rho-\rho S_3^+S_3^-) \tag{14}$$

is the damping operator for the atom. Here, $\Delta_c=\omega_c-\omega_L$ and $\Delta_a=\omega_{12}-\omega_L$ are the detunings of the cavity-mode frequency ω_c and of the atomic transition frequency ω_{12} from the driving field frequency ω_L; $\Delta_p=\omega_{32}-\omega_p$ is the detuning of the probe field from the $|2\rangle-|3\rangle$ transition, $S_3^+=|3\rangle\langle 2|$, $S_3^-=|2\rangle\langle 3|$ are the atomic dipole operators of the $|3\rangle-|2\rangle$ transition, $\Omega(\Omega_p)$ is the Rabi frequency of the driving (probe) field, and κ,Γ_1,Γ_3 are the cavity and spontaneous-emission damping rates.

The master equation (10) describes the time evolution of the atom plus cavity system and contains all the essential incoherent and coherent effects of atomic spontaneous emission, cavity damping, atom-cavity coupling, and the driving field. The equation has been extensively employed to investigate the fundamentals of the CQED, and the theoretical studies are usually performed in the so-called ''bad cavity'' and ''good cavity'' limits. The limits are determined by two relations between the parameters g, κ, and Γ_1. The bad cavity limit corresponds to $\kappa\gg g,\Gamma_1$, in which the cavity damping dominates, whereas the good cavity limit with $g\gg\kappa,\Gamma_1$ corresponds to a strong atom-cavity coupling in which the atom-cavity interaction dominates over that leading to the atomic and cavity decay.

In this paper we are interested in the good cavity limit in which the photon emitted by the atom into the cavity mode is likely to be repeatedly exchanged between these two systems before reaching the stationary state. Moreover, we assume that the Rabi frequency of the driving field is so strong that

$$\Omega\gg\kappa,\Gamma_1,\Gamma_3, \tag{15}$$

and the laser and cavity frequencies are resonant to the atomic transition, $\Delta_c=\Delta_a=0$.

Since the $|2\rangle-|1\rangle$ transition is strongly driven by the laser field, it is convenient to work in the basis of the semiclassical dressed states of the transition [20]

$$|d_1\rangle=\frac{1}{\sqrt{2}}(|2\rangle+|1\rangle),$$

$$|d_2\rangle=\frac{1}{\sqrt{2}}(|2\rangle-|1\rangle). \tag{16}$$

In the dressed-atom approach we express the atomic operators $S_i^{\pm}$ in terms of dressed-state operators $R_{ij}=|d_i\rangle\langle d_j|$ as

$$S_1^+=\frac{1}{2}(R_0-R_{12}+R_{21}),$$

$$S_1^-=\frac{1}{2}(R_0-R_{21}+R_{12}),$$

$$S_3^+=\frac{1}{\sqrt{2}}(R_{32}+R_{31}), \tag{17}$$

where $R_0=R_{22}-R_{11}$.

Next, we substitute Eq. (17) into Eq. (10) and find that the master equation can be written as

$$\frac{d\rho}{dt}=-\frac{i}{\hbar}[\tilde{H}_c+\tilde{H}_L+\tilde{H}_p,\rho]+L_c\rho+\tilde{L}_a\rho,$$

where

$$\tilde{H}_c=\frac{1}{2}ig\hbar[a^\dagger(R_0-R_{21}+R_{12})-\text{H.c.}], \tag{18}$$

$$\tilde{H}_p=\frac{\Omega_p}{2\sqrt{2}}(R_{32}+R_{31}+\text{H.c.}), \tag{19}$$

$$\tilde{H}_L=\hbar\left(\Delta_c a^\dagger a+\frac{1}{2}\Omega R_0\right), \tag{20}$$

and

$$\begin{aligned}\tilde{L}_a\rho=&\frac{1}{4}\Gamma_1(R_0-R_{21}+R_{12})\rho(R_0-R_{12}+R_{21})\\&-\frac{1}{8}\Gamma_1(R_0-R_{12}+R_{21})(R_0-R_{21}+R_{12})\rho\\&-\frac{1}{8}\Gamma_1\rho(R_0-R_{12}+R_{21})(R_0-R_{21}+R_{12})\\&+\frac{1}{2}\Gamma_3(R_{23}+R_{13})\rho(R_{32}+R_{31})-\frac{1}{4}\Gamma_3(R_{32}+R_{31})(R_{23}\\&+R_{13})\rho-\frac{1}{4}\Gamma_3\rho(R_{32}+R_{31})(R_{23}+R_{13}).\end{aligned} \tag{21}$$

For high-field strengths, $\Omega\gg\Gamma_1,\Gamma_3,\kappa$, an approximation technique has been suggested [7] which greatly simplifies the damping term (21). In this approach, we define the new (transformed) density operator

$$\tilde{\rho}(t)=e^{-(i/\hbar)\tilde{H}_Lt}\rho e^{(i/\hbar)\tilde{H}_Lt}, \tag{22}$$

and find that the transformed density operator satisfies the following master equation:

$$\frac{d}{dt}\tilde{\rho}(t)=-\frac{i}{\hbar}[\tilde{H}_c(t)+\tilde{H}_p(t),\tilde{\rho}(t)]+\mathcal{L}_c\tilde{\rho}(t)+\mathcal{L}_a\tilde{\rho}(t), \tag{23}$$

where

$$\begin{aligned}\tilde{H}_c(t)=&\frac{1}{2}ig\hbar[a^\dagger(R_0e^{i\Delta_ct}-R_{21}e^{i(\Delta_c+\Omega)t}\\&-R_{12}e^{i(\Delta_c-\Omega)t})-\text{H.c.}],\end{aligned}$$

$$\tilde{H}_p(t)=\frac{\Omega_p}{2\sqrt{2}}(R_{32}e^{(1/2)i\Omega t}+R_{31}e^{-(1/2)i\Omega t}+\text{H.c.}), \tag{24}$$

and

$$\begin{aligned}\tilde{L}_a\tilde{\rho}(t)=&\frac{1}{4}\Gamma_1(R_0-R_{21}e^{i\Omega t}+R_{12}e^{-i\Omega t})\tilde{\rho}(t)(R_0-R_{12}e^{-i\Omega t}\\&+R_{21}e^{i\Omega t})-\frac{1}{8}\Gamma_1(R_0-R_{12}e^{-i\Omega t}+R_{21}e^{i\Omega t})\\&\times(R_0-R_{21}e^{i\Omega t}+R_{12}e^{-i\Omega t})\tilde{\rho}(t)-\frac{1}{8}\Gamma_1\tilde{\rho}(t)\\&\times(R_0-R_{12}e^{i\Omega t}+R_{21}e^{i\Omega t})\\&\times(R_0-R_{21}e^{i\Omega t}+R_{12}e^{-i\Omega t})+\frac{1}{2}\Gamma_3\\&\times(R_{23}+R_{13}e^{i\Omega t})\tilde{\rho}(t)(R_{32}+R_{31}e^{-i\Omega t})-\frac{1}{4}\Gamma_3\\&\times(R_{32}+R_{31}e^{-i\Omega t})(R_{23}+R_{13}e^{i\Omega t})\tilde{\rho}(t)-\frac{1}{4}\Gamma_3\tilde{\rho}(t)\\&\times(R_{32}+R_{31}e^{-i\Omega t})(R_{23}+R_{13}e^{i\Omega t}).\end{aligned} \tag{25}$$

It is seen from Eqs. (24) and (25) that certain terms of the master equation are independent of time while others vary in time with Δ_c, $\Delta_c\pm\Omega$, and $\pm\Omega$. Depending on the cavity detuning, some of the oscillating terms may slowly vary in time. Here we assume that $\Delta_c=0$, and then dropping the terms oscillating rapidly at $\pm\Omega$ and $\pm2\Omega$ the master equation (23) reduces to

$$\frac{d}{dt}\tilde{\rho}(t)=\frac{1}{2}g[a^{\dagger}R_0-R_0a,\tilde{\rho}(t)]-\frac{i}{\hbar}[\tilde{H}_p(t),\tilde{\rho}(t)]+L_c\tilde{\rho}(t)$$
$$-\frac{1}{8}\Gamma_1(R_0^2\tilde{\rho}(t)+\tilde{\rho}(t)R_0^2-2R_0\tilde{\rho}(t)R_0)$$
$$-\frac{1}{8}\Gamma_1(R_{12}R_{21}\tilde{\rho}(t)+\tilde{\rho}(t)R_{12}R_{21}-2R_{21}\tilde{\rho}(t)R_{12})$$
$$-\frac{1}{8}\Gamma_1(R_{21}R_{12}\tilde{\rho}(t)+\tilde{\rho}(t)R_{21}R_{12}-2R_{12}\tilde{\rho}(t)R_{21})$$
$$-\frac{1}{4}\Gamma_3(R_{31}R_{13}\tilde{\rho}(t)+\tilde{\rho}(t)R_{31}R_{13}-2R_{13}\tilde{\rho}(t)R_{31})$$
$$-\frac{1}{4}\Gamma_3(R_{32}R_{23}\tilde{\rho}(t)+\tilde{\rho}(t)R_{32}R_{23}-2R_{23}\tilde{\rho}(t)R_{32}). \tag{26}$$

It should be pointed out here that the master equation (26) is diagonal in respect to the driving field, but nondiagonal in respect to the cavity field. Therefore the secular approximation used in the derivation of Eq. (26) is valid only when the Rabi frequency $\Omega_c=2g\sqrt{\langle n\rangle}$ of the cavity field is much smaller than the Rabi frequency of the driving field. In other words, the cavity field produces oscillations which are much slower than those produced by the driving field. When $\Omega_c \approx \Omega$ the atomic dynamics can change dramatically, and we will address this point in Sec. VI. In the next section we will apply the master equation (26) to calculate the Autler-Townes spectrum for this system.

IV. THE AUTLER-TOWNES SPECTROSCOPY

In Autler-Townes spectroscopy, the absorptive properties of a system are studied by monitoring the system with a weak probe field coupled to an auxiliary level. The population of the auxiliary level is measured as a function of the probe field frequency, or equivalently, one can measure the coherence between the auxiliary level and one of the probed levels. We present arguments below which demonstrate that the dominant features of the Autler-Townes spectrum are determined by the populations of the dressed states, $\rho_{d_id_i}$.

First we calculate the population of the state $|3\rangle$ as a function of the probe field detuning Δ_p. From the master equation (26), we find that the equations of motion for the population of the state $|3\rangle$ and the coherences between state $|3\rangle$ and the dressed states $|d_1\rangle$ and $|d_2\rangle$ are given by

$$\tilde{\rho}_{33}=-\Gamma_3\tilde{\rho}_{33}+\frac{\Omega_p}{2\sqrt{2}}(\tilde{\rho}_{3d_1}+\tilde{\rho}_{3d_2}+\tilde{\rho}_{d_13}+\tilde{\rho}_{d_23})+L_c\tilde{\rho}_{33}, \tag{27}$$

$$\tilde{\rho}_{3d_1}=-\left[\frac{1}{2}\left(\Gamma_3+\frac{1}{2}\Gamma_1\right)+i\left(\Delta_p-\frac{1}{2}\Omega\right)\right]\tilde{\rho}_{3d_1}$$
$$-\frac{1}{2}g\tilde{\rho}_{3d_1}(a-a^{\dagger})+\frac{\Omega_p}{2\sqrt{2}}(\tilde{\rho}_{d_1d_1}-\tilde{\rho}_{33})+L_c\tilde{\rho}_{3d_1},$$

$$\tilde{\rho}_{3d_2}=-\left[\frac{1}{2}\left(\Gamma_3+\frac{1}{2}\Gamma_1\right)+i\left(\Delta_p+\frac{1}{2}\Omega\right)\right]\tilde{\rho}_{3d_2}$$
$$-\frac{1}{2}g\tilde{\rho}_{3d_2}(a-a^{\dagger})+\frac{\Omega_p}{2\sqrt{2}}(\tilde{\rho}_{d_2d_2}-\tilde{\rho}_{33})+L_c\tilde{\rho}_{3d_2}.$$

Equations (27) are still operators with respect to the cavity field. Since the probe field is very weak, the population $\tilde{\rho}_{33}$ is much smaller than the populations $\tilde{\rho}_{d_2d_2}$ and $\tilde{\rho}_{d_1d_1}$ and we can ignore the effect of $\tilde{\rho}_{33}$ on the evolution of the coherences $\tilde{\rho}_{3d_1}$ and $\tilde{\rho}_{3d_2}$.

In the absence of the cavity, the density-matrix elements (27) become c numbers and it is easy to find that the steady-state population $\tilde{\rho}_{33}$ is given by

$$\tilde{\rho}_{33}=\frac{\Omega_p^2}{8\Gamma_3}\left[\frac{(\Gamma_3+\frac{1}{2}\Gamma_1)\tilde{\rho}_{d_1d_1}}{\frac{1}{4}(\Gamma_3+\frac{1}{2}\Gamma_1)^2+(\Delta_p-\frac{1}{2}\Omega)^2}\right.$$
$$\left.+\frac{(\Gamma_3+\frac{1}{2}\Gamma_1)\tilde{\rho}_{d_2d_2}}{\frac{1}{4}(\Gamma_3+\frac{1}{2}\Gamma_1)^2+(\Delta_p+\frac{1}{2}\Omega)^2}\right], \tag{28}$$

which is the familiar Autler-Townes doublet. The spectrum is composed of two lines of equal linewidths, $\frac{1}{2}(\Gamma_3+\frac{1}{2}\Gamma_1)$, and located at the frequencies $\pm\frac{1}{2}\Omega$. The intensities of the lines are proportional to the populations of the dressed states and are equal when $\tilde{\rho}_{d_1d_1}=\tilde{\rho}_{d_2d_2}$, while the intensities are unequal when $\tilde{\rho}_{d_1d_1}\neq\tilde{\rho}_{d_2d_2}$.

In the presence of the cavity, and in the photon-number representation, we find that the coherence $X_{n,m}=\langle n|\tilde{\rho}_{3d_1}|m\rangle$ satisfies the recurrence relation

$$A_{n,m}X_{n,m}+\frac{1}{2}g\sqrt{m}X_{n,m-1}-\frac{1}{2}g\sqrt{m+1}X_{n,m+1}$$
$$+\kappa\sqrt{(n+1)(m+1)}X_{n+1,m+1}=\frac{\Omega_p}{2\sqrt{2}}\tilde{\rho}_{n,m}^{(d_1d_1)}, \tag{29}$$

where

$$A_{n,m}=\frac{1}{2}\left(\Gamma_3+\frac{1}{2}\Gamma_1\right)+\frac{1}{2}\kappa(n+m)+i\left(\Delta_p-\frac{1}{2}\Omega\right) \tag{30}$$

and $\tilde{\rho}_{n,m}^{(d_1d_1)}=\langle n|\tilde{\rho}_{d_1d_1}|m\rangle$. The recurrence relation for the coherence $Y_{n,m}=\langle n|\tilde{\rho}_{3d_2}|m\rangle$ has the same form as Eq. (29) with $\Omega\rightarrow-\Omega$ and $d_1\rightarrow d_2$.

In general, Eq. (29) is a two-dimensional recurrence relation and reduces to a one-dimensional recurrence relation in the limit of vanishing cavity damping $\kappa\rightarrow0$. The coherences $X_{n,m}$ depend on the population $\tilde{\rho}_{n,m}^{(d_1d_1)}$ of the cavity-modified dressed states and are also coupled to the ''nondiagonal'' elements $X_{n,m\pm1}$ and $X_{n+1,m+1}$. In the lowest order of cou-

pling, in which we ignore the coupling of the diagonal elements to the off-diagonal elements, the coherence $X_{n,m}$ is given by

$$X_{n,m}=\frac{\Omega_p}{2\sqrt{2}}\frac{\tilde{\rho}_{n,m}^{(d_1d_1)}}{A_{n,m}}, \tag{31}$$

which is similar to the free-space case.

In the next approximation, we include the coupling of $X_{n,m}$ to $X_{n,m\pm1}$, and we find that near the resonance $\Delta_p \approx \frac{1}{2}\Omega$, and for small cavity damping, the coherence is given by

$$X_{n,m}=\frac{\Omega_p}{2\sqrt{2}}\frac{\tilde{\rho}_{n,m}^{(d_1d_1)}}{\frac{1}{2}(\Gamma_3+\frac{1}{2}\Gamma_1)+\dfrac{2g^2n}{(\Gamma_3+\frac{1}{2}\Gamma_1)}+i(\Delta_p-\frac{1}{2}\Omega)}. \tag{32}$$

It is seen that the effect of the off-diagonal terms is to produce a power broadening of the Autler-Townes lines. Thus, as in the case of free space, the major factor determining the shape and intensities of the Autler-Townes lines is the population distribution between the dressed states of the driven transition. We describe how to calculate these in the next section.

V. POPULATION OF THE DRESSED STATES

From the master equation (26), we find that the equations of motion for the populations of the dressed states are of the form

$$\begin{aligned}\dot{\rho}_{11}&=\frac{1}{2}g[(a-a^\dagger)\rho_{11}-\rho_{11}(a-a^\dagger)]-\frac{1}{4}\Gamma_1(\rho_{11}-\rho_{22})\\&\quad+L_c\rho_{11},\\ \dot{\rho}_{22}&=-\frac{1}{2}g[(a-a^\dagger)\rho_{22}-\rho_{22}(a-a^\dagger)]-\frac{1}{4}\Gamma_1(\rho_{22}-\rho_{11})\\&\quad+L_c\rho_{22},\end{aligned} \tag{33}$$

where $\rho_{ii}=\tilde{\rho}_{d_id_i}$. It is interesting to note that the equations of motion for the populations are decoupled from the equations of motion for the coherences, which are given by

$$\begin{aligned}\dot{\rho}_{12}&=-ig(a\rho_{12}-\rho_{12}a^\dagger)-\frac{3}{4}\Gamma_1\rho_{12}+L_c\rho_{12},\\ \dot{\rho}_{21}&=-ig(a\rho_{21}-\rho_{21}a^\dagger)-\frac{3}{4}\Gamma_1\rho_{21}+L_c\rho_{21}.\end{aligned} \tag{34}$$

Thus, Eqs. (33) and (34) form independent coupled pairs.

It is convenient to introduce the following combinations of the dressed-states populations:

$$\begin{aligned}u&=\rho_{11}+\rho_{22},\\ w&=\rho_{22}-\rho_{11}.\end{aligned} \tag{35}$$

From Eq. (33) we find that the equations of motion for the combinations u and w are

$$\dot{u}=-\frac{1}{2}g[(a-a^\dagger)w-w(a-a^\dagger)]+L_cu, \tag{36}$$

$$\dot{w}=-\frac{1}{2}g[(a-a^\dagger)u-u(a-a^\dagger)]-\frac{1}{2}\Gamma_1w+L_cw. \tag{37}$$

Note that $u=\mathrm{Tr}_{atom}(\rho)$ is the reduced density operator of the cavity field.

In the photon-number representation, the equations of motion for $u_{n,m}=\langle n|u|m\rangle$ and $w_{n,m}=\langle n|w|m\rangle$ are given by

$$\begin{aligned}\dot{u}_{n,m}&=-\frac{1}{2}g\sqrt{n+1}w_{n+1,m}+\frac{1}{2}g\sqrt{n}w_{n-1,m}+\frac{1}{2}g\sqrt{m}w_{n,m-1}\\&\quad-\frac{1}{2}g\sqrt{m+1}w_{n,m+1}+\kappa\sqrt{(n+1)(m+1)}u_{n+1,m+1}\\&\quad-\frac{1}{2}\kappa(n+m)u_{n,m},\\ \dot{w}_{n,m}&=-\frac{1}{2}g\sqrt{n+1}u_{n+1,m}+\frac{1}{2}g\sqrt{n}u_{n-1,m}+\frac{1}{2}g\sqrt{m}u_{n,m-1}\\&\quad-\frac{1}{2}g\sqrt{m+1}u_{n,m+1}+\kappa\sqrt{(n+1)(m+1)}w_{n+1,m+1}\\&\quad-\frac{1}{2}\kappa(n+m)w_{n,m}-\frac{1}{2}\Gamma_1w_{n,m}.\end{aligned} \tag{38}$$

It is seen from Eq. (38) that the diagonal elements $u_{n,m}(w_{n,m})$ are coupled to the off-diagonal elements $w_{n\pm1,m}(u_{n\pm1,m})$ and $w_{n,m\pm1}(u_{n,m\pm1})$. By setting the left-hand side of Eq. (38) equal to zero we obtain the steady-state solutions of these equations. A straightforward manipulation of Eq. (38) leads to the following six-term two-dimensional recurrence relation:

$$\begin{aligned}&G_{n,m}Z^{(n,m)}+D_{n+1,m+1}Z^{(n+1,m+1)}+B_{0,m+1}Z^{(n,m+1)}\\&\quad+B_{n+1,0}Z^{(n+1,m)}-B_{0,m}Z^{(n,m-1)}-B_{n,0}Z^{(n-1,m)}=0,\end{aligned} \tag{39}$$

where

$$\begin{aligned}Z^{(n,n)}&=\begin{pmatrix}u^{(n,m)}\\ w^{(n,m)}\end{pmatrix},\quad G_{n,m}=\begin{pmatrix}\kappa n & 0\\ 0 & \kappa n+\frac{1}{2}\Gamma_1\end{pmatrix},\\ B_{n,m}&=\begin{pmatrix}0 & g\sqrt{n+m}\\ g\sqrt{n+m} & 0\end{pmatrix},\\ D_{n,m}&=\begin{pmatrix}-\kappa\sqrt{nm} & 0\\ 0 & -\kappa\sqrt{nm}\end{pmatrix},\end{aligned} \tag{40}$$

with $\Sigma_{n,m}u_{n,m}=1$. Note that the degeneracy in the cavity and driving field frequencies leads to a doubling of the dimension

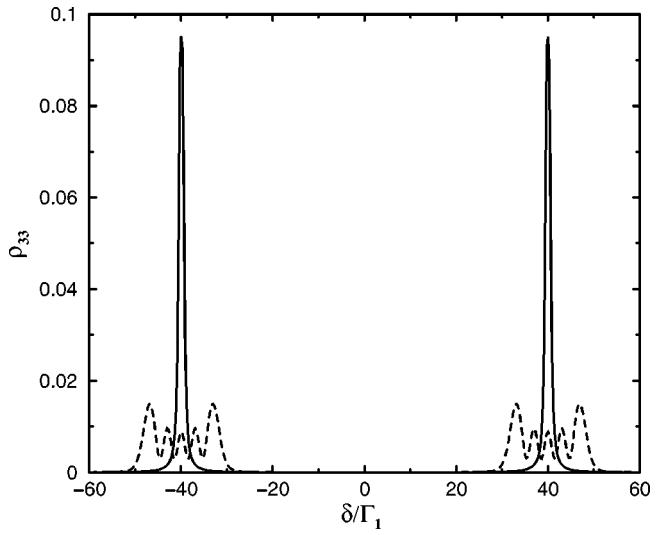

FIG. 3. The Autler-Townes spectrum for $\Omega=80\Gamma_1$, $\kappa=\Gamma_3=0.1\Gamma_1$, and different atom-cavity couplings: $g=0.01\Gamma_1$ (solid line), $g=1.5\Gamma_1$ (dashed line).

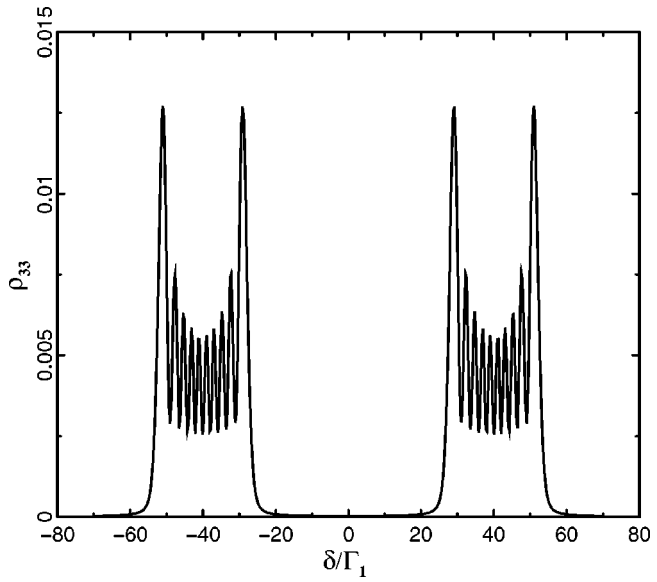

FIG. 4. The Autler-Townes spectrum for $\Omega=80\Gamma_1$, $\kappa=0.01\Gamma_1$, $\Gamma_3=0.1\Gamma_1$, and $g=2\Gamma_1$.

of the dynamics of the system, in the sense that the diagonal elements $u_{n,n}(w_{n,n})$ are not decoupled from the off-diagonal elements $u_{n,n+m}(w_{n,n+m})$. To obtain the Autler-Townes absorption spectrum, we calculate the steady-state coherence ρ_{32} from the recurrence relation (29) with the populations found from the recurrence relation (39), and then find the population ρ_{33} as a function of Δ_p.

VI. RESULTS AND DISCUSSION

In order to see the modifications in the dynamics of the driven atomic transition produced by the cavity, we concentrate on the strong field limit of $\Omega\gg\Gamma_1,\Gamma_3,\kappa$. We employ two separate approaches: In the first method, we calculate the Autler-Townes spectrum in a truncated basis which assumes that there is a small, fixed number of photons in the cavity mode. These results of this approach are shown in Figs. 3–5. Recent experiments [23] have shown that it is possible to produce Fock states in the one-atom maser with up to seven photons present. In the second approach, we calculate the spectrum assuming a basis set with a large number of photons. Here the external driving field produces a photon number distribution in the cavity.

A. The case of a fixed number of photons in the cavity

In Fig. 3 we show the steady-state population ρ_{33} as a function of the detuning Δ_p. For $g\ll\kappa,\Gamma_1$, shown as a solid line, the spectrum displays two peaks located at $\pm\frac{1}{2}\Omega$. This is the well-known Autler-Townes doublet consisting of two lines of linewidth $\frac{1}{2}(\Gamma_3+\frac{1}{2}\Gamma_1)$ and separated by the Rabi frequency Ω of the driving field. As the coupling constant g increases the lines broaden and for $g\gg\kappa,\Gamma_1$, split into multiplets. The width of the spectral lines and the number of peaks depend on g, which determines the Rabi frequency of the cavity field. In Fig. 4 we plot the spectrum for $g=2\Gamma_1$, $\kappa=0.01\Gamma_1$, $\Omega=80\Gamma_1$, and $\Gamma_3=0.1\Gamma_1$. This plot corresponds to a larger number of photons in the cavity mode, $n=7$. We see that the splitting of the spectral features and the number of lines inside the structures increase with increasing n. From Figs. 3 and 4 it is apparent that the splitting of the features is proportional to $2g\sqrt{n}$, i.e., the Rabi frequency of the cavity field. Figure 5 shows the spectrum for two different values of n and g such that $2g\sqrt{n}=\text{const}$. Here we see that the number of peaks in the structures increases with n and the oscillations vanish for a large n. The case of $n\gg1$ corresponds to the Autler-Townes spectrum of a two-level transition driven by two lasers of the same frequencies [21].

The multipeak structure of the Autler-Townes spectrum could suggest that in the presence of the cavity the dressed

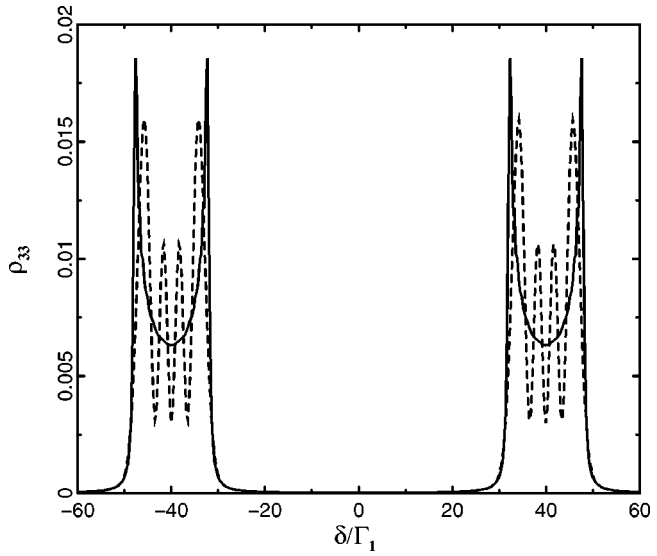

FIG. 5. The Autler-Townes spectrum for $\Omega=80\Gamma_1$ and the other parameters chosen such that $g\sqrt{n}=\text{const}$: $g=0.666\Gamma_1$, $n=36$ (solid line), $g=2\Gamma_1$, $n=4$ (dashed line).

states $|d_1\rangle$ and $|d_2\rangle$ split into multiplets. However, this is not the case in the present system, as the fully quantized analysis of Sec. II demonstrates. There it was shown that the energy-level spectrum of the system was composed of an infinite ladder of doublet continua with interdoublet separation ω_{12} and intradoublet separation Ω. The dressed-state eigenfunctions were linear combinations of the eigenfunctions $\phi_n(x)$ of the harmonic oscillator.

Thus a weak laser field coupled to the $|3\rangle-|2\rangle$ transition will probe the steady-state population distribution in the continua induced by the cavity and driving laser fields. In order to find the steady-state population of the dressed states (8) we project the master equation (10) onto $|N,d_i,\lambda\rangle$ on the right and $\langle N,d_i,\lambda|$ on the left. We make the secular approximation [20] valid for $\Omega \gg \Gamma_1,\Gamma_3$, in which we ignore the coupling of the populations to the coherences, and find that the ''reduced'' steady-state populations $P_{d_i}=\Sigma_N\langle N,d_i,\lambda|\rho|N,d_i,\lambda\rangle$ are

$$P_{d_i}=\frac{1}{2}\left|\phi_n\left(\frac{\lambda}{\sqrt{2}}\right)\right|^2. \tag{41}$$

The population is distributed equally between the continua of the dressed states and is spread across these states with the weight function $|\phi_n(\lambda/\sqrt{2})|^2$. Clearly the oscillations seen in Figs. 3–5 result from the oscillatory distribution of the population inside the continuum of the dressed states. The oscillations provide direct evidence of field quantization in the cavity and their observation would provide a measurement of the probability distribution function of the harmonic oscillator, with $\lambda/\sqrt{2}$ playing the role of the harmonic-oscillator coordinate.

B. The case of a variable number of cavity photons in the basis

The second approach has been used to obtain Fig. 6, which shows the Autler-Townes spectrum for $\Omega=100\Gamma_1$, $\kappa=0.1\Gamma_1$, $\Gamma_3=0.1\Gamma_1$, and different g. This spectrum has been obtained using a truncated basis of 70 number states. One sees that for small g the spectrum is the familiar Autler-Townes doublet. For moderate g the spectral lines split into multiplets with the overall width of the features equal to the Rabi frequency of cavity field $\Omega_c=2g\sqrt{\langle n\rangle}$, where $\langle n\rangle$ is the average number of photons in the cavity mode. The width of the multiple structures increases linearly with g indicating that the average number of photons in the cavity mode is constant, independent of g. Surprisingly, for large g the splitting disappears and the Autler-Townes multiple doublet reduces to a single peak with linewidth approximately equal to Γ_3, located at the atomic transition frequency ω_{12}. We have found that there is a threshold value of g at which the Autler-Townes splitting disappears. The threshold value corresponds to $\Omega_c=\Omega$.

In order to get a physical insight into the cancellation of the Autler-Townes splitting, we plot in Fig. 7 the quantity $\mathrm{Tr}(\rho^2)$ which provides information about the number of states of the system and their purity. We find $\mathrm{Tr}(\rho^2)$ by

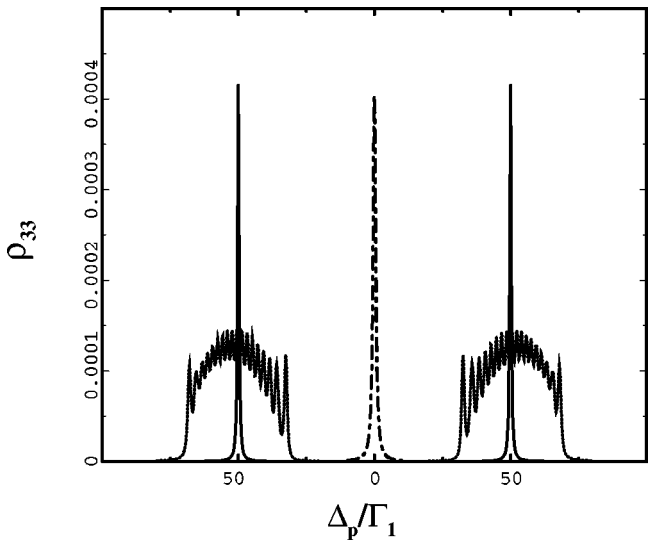

FIG. 6. The Autler-Townes spectrum for $\Omega=100\Gamma_1$, $\kappa=\Gamma_3=0.1\Gamma_1$, and different g: $g=0.01\Gamma_1$ (solid line), $g=3\Gamma_1$ (dotted line), $g=20\Gamma_1$ (dashed-dotted line).

direct integration of the master equation (10). In this approach we use the Fock state representation for the cavity field and write the density matrix ρ as a vector composed of the density-matrix elements. We solve this system of linear, ordinary, differential equations by using numerical methods available for Matlab [19].

In the absence of the cavity ($g=0$), $\mathrm{Tr}(\rho^2)=\frac{1}{2}$ indicating that the system is in a mixed state of the two dressed states $|d_1\rangle$ and $|d_2\rangle$. In the presence of the cavity and for small g the state of the system becomes more mixed with $\mathrm{Tr}(\rho^2)\approx 0$. This indicates that the system is in a mixed state with a very large number of states. This is easy to understand if one refers to Eq. (7) which shows that the energy spectrum of the system is composed of two continua, each containing an in-

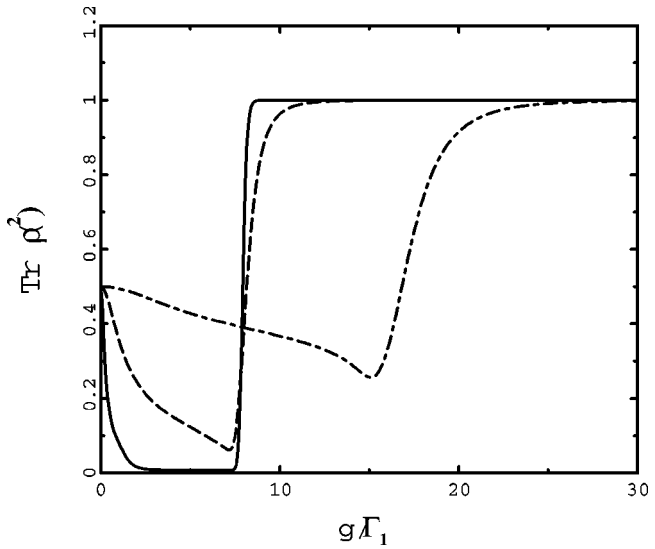

FIG. 7. $\mathrm{Tr}(\rho^2)$ as a function of g for $\kappa=\Gamma_3=0.1\Gamma_1$ and $\Omega=100\Gamma_1$.

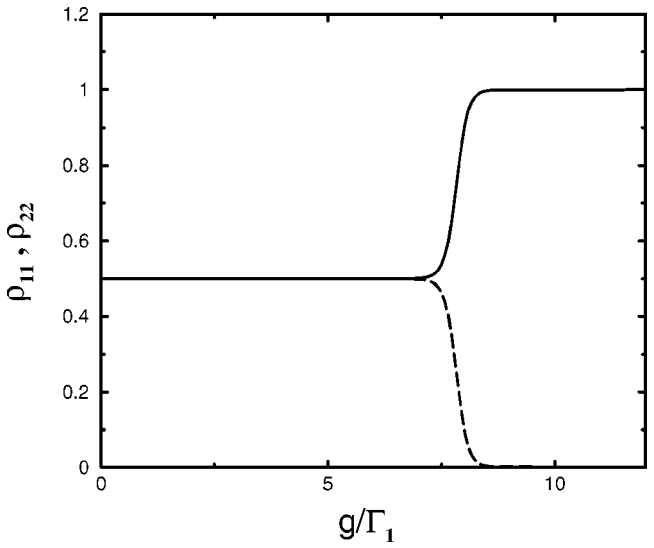

FIG. 8. Populations of the atomic bare states as a function of g for the same parameters as in Fig. 7: ρ_{22} (solid line), ρ_{11} (dashed line).

finite number of states. As g increases the purity remains constant and at $g \approx 7.5$ changes rapidly from the maximally mixed state $\mathrm{Tr}(\rho^2)=0$ to a maximally pure state $\mathrm{Tr}(\rho^2)=1$. For $g>7.5$ the system independent of g remains in the pure state. In Fig. 8 we plot the populations of the atomic bare states $|1\rangle$ and $|2\rangle$ for the same parameters as in Fig. 7. We see that for $g<7.5$ the atomic states are equally populated and the population does not change with g. When $g \approx 7.5$ the atom collapses into its ground state and remains in this state, independent of g.

Alsing *et al.* [10] have predicted that a two-level atom located inside a lossless cavity can remain in its ground state even if is continuously driven by a coherent laser field. They have explained this effect as arising from the destructive interference between the driving and the cavity fields which cancels the effective driving of the atom. Here, we present an alternative and more transparent explanation which involves linear superpositions of two degenerate dressed states of the system. The degeneracy appears only when $\Omega_c \geqslant \Omega$.

According to Fig. 2, the continua are separated by $\Omega - \Omega_c$ and they start to overlap when $\Omega_c = \Omega$. In the case of nonoverlapping continua the only nonvanishing dipole matrix elements are between two neighboring manifolds and are given by

$$\langle N,d_1,\lambda|\vec{\mu}|N-1,d_2,\lambda'\rangle = \frac{1}{2}\vec{\mu}_{12}\delta(\lambda+\lambda'),$$

$$\langle N,d_2,\lambda|\vec{\mu}|N-1,d_1,\lambda'\rangle = -\frac{1}{2}\vec{\mu}_{12}\delta(\lambda+\lambda'),$$

$$\langle N,d_1,\lambda|\vec{\mu}|N-1,d_1,\lambda'\rangle = \frac{1}{2}\vec{\mu}_{12}\delta(\lambda-\lambda'),$$

$$\langle N,d_2,\lambda|\vec{\mu}|N-1,d_2,\lambda'\rangle = -\frac{1}{2}\vec{\mu}_{12}\delta(\lambda-\lambda'). \quad (42)$$

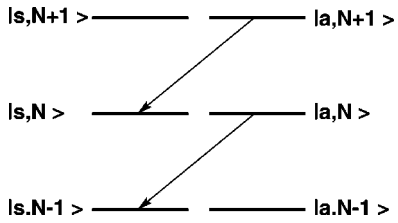

FIG. 9. Superpositions states of the overlapping continua. The solid arrows indicate the allowed spontaneous transitions.

Consider two extremal states of the continua $|N,d_1,\lambda_{max}\rangle$ and $|N,d_2,\lambda_{min}\rangle$ which overlap for $\Omega_c=\Omega$. The degeneracy in the energy of the two overlapping states leads to the following linear superposition states

$$|s,N\rangle = \frac{1}{\sqrt{2}}(|N,d_1,\lambda_{max}\rangle + |N,d_2,\lambda_{min}\rangle),$$

$$|a,N\rangle = \frac{1}{\sqrt{2}}(|N,d_1,\lambda_{max}\rangle - |N,d_2,\lambda_{min}\rangle). \quad (43)$$

It is easily verified from Eqs. (42) and (43) that the *only* nonzero transition moments are between the states $|a,N+p\rangle$ and $|s,N+p-1\rangle$

$$\langle N+p,a|\vec{\mu}|s,N+p-1\rangle = \frac{1}{4}\vec{\mu}_{12}, \quad (44)$$

where $p=0,1,2,\ldots$. In Fig. 9 we plot the superposition states and the allowed spontaneous transitions. It is clear from Fig. 9 that the population flows from the antisymmetric state to the symmetric state of the manifold below but cannot escape from the symmetric state, resulting in the trapping of the population in that state.

Using Eqs. (43) it is easy to show that the symmetric state can be written as

$$|s,N\rangle = \sum_n \phi_n(\lambda_{max}/\sqrt{2})|2,N-n,n\rangle. \quad (45)$$

Thus, the trapping state of the system involves only the ground state of the atom.

VII. SUMMARY

We have demonstrated the relation between the harmonic oscillator and a two-level atom coupled to a cavity mode and driven by a resonant laser field. The properties of this system have been investigated by connecting the ground state to a third level, not coupled to the cavity, by a weak probe field, and calculating the Autler-Townes spectrum. In the strong-coupling limit the components of the Autler-Townes doublet are composed of multiplets, whose detailed structure depends on the atom-cavity coupling and the cavity and spontaneous-emission damping rates. We have shown that the multiplets do not correspond to any discrete energy levels of the system, but result from the oscillatory distribution of the population inside the continuum of the dressed states.

The oscillations, which are a signature of the quantum nature of the cavity field, are a direct analog of the well-known oscillations of the probability distribution function of the harmonic oscillator, and should be measurable for this system. The probability distribution function of the harmonic oscillator has not yet been measured, and it is obviously of great interest to observe this fundamental property. We have also shown that there is a threshold value for the Rabi frequency of the cavity field at which the Autler-Townes splitting disappears and the atom collapses to the ground state, and interpreted it as a population trapping effect.

ACKNOWLEDGMENT

This research was supported by the United Kingdom Engineering and Physical Sciences Research Council.

[1] J. Ye, D.W. Vernooy, and H.J. Kimble, Phys. Rev. Lett. **83**, 4987 (1999); A.C. Doherty, T.W. Lynn, C.J. Hood, and H.J. Kimble, Phys. Rev. A **63**, 013401 (2001).
[2] A. Whitaker, Prog. Quantum Electron. **24**, 1 (2000).
[3] E.T. Jaynes and F.W. Cummings, Proc. IEEE **51**, 89 (1963).
[4] J.H. Eberly, N.B. Narozhny, and J.I. Sanchez-Mondragon, Phys. Rev. Lett. **44**, 1323 (1980); P.L. Knight and P.M. Radmore, Phys. Lett. **90A**, 342 (1982); G. Rempe, H. Walther, and N. Klein, Phys. Rev. Lett. **58**, 353 (1987).
[5] H.J. Carmichael, R.J. Brecha, M.G. Raizen, H.J. Kimble, and P.R. Rice, Phys. Rev. A **40**, 5516 (1989).
[6] J.I. Cirac, H. Ritsch, and P. Zoller, Phys. Rev. A **44**, 4541 (1991).
[7] T. Quang and H. Freedhoff, Phys. Rev. A **47**, 2285 (1993); H. Freedhoff and T. Quang, J. Opt. Soc. Am. B **10**, 1337 (1993); Phys. Rev. Lett. **72**, 474 (1994).
[8] R.J. Brecha, P.R. Rice, and M. Xiao, Phys. Rev. A **59**, 2392 (1999); J.P. Clemens and P.R. Rice, *ibid.* **61**, 063810 (2000).
[9] C.M. Savage, Phys. Rev. Lett. **60**, 1828 (1988); M. Lindberg and C.M. Savage, Phys. Rev. A **38**, 5182 (1988); C.M. Savage, Phys. Rev. Lett. **63**, 1376 (1989); P. Alsing and H.J. Carmichael, Quantum Opt. **3**, 13 (1991); P.M. Alsing, D.-S. Guo, and H.J. Carmichael, Phys. Rev. A **45**, 5135 (1992); H. Nha, Y.-T. Chough, and K. An, *ibid.* **62**, 021801(R) (2000).
[10] P.M. Alsing, D.A. Cardimona, and H.J. Carmichael, Phys. Rev. A **45**, 1793 (1992).
[11] B.R. Mollow, Phys. Rev. **188**, 1969 (1969).
[12] M. Lewenstein, T.W. Mossberg, and R.J. Glauber, Phys. Rev. Lett. **59**, 775 (1987); M. Lewenstein and T.W. Mossberg, Phys. Rev. A **37**, 2048 (1988); P. Zhou and S. Swain, *ibid.* **58**, 1515 (1998).
[13] M. Brune, F. Schmidt-Kaler, A. Maali, J. Dreyer, E. Hagley, J.M. Raimond, and S. Haroche, Phys. Rev. Lett. **76**, 1800 (1996).
[14] B.T.H. Varcoe, S. Brattke, B.G. Englert, and H. Walther, Laser Phys. **10**, 1 (2000); B.T.H. Varcoe, S. Brattke, M. Weldinger, and H. Walther, Nature (London) **403**, 743 (2000); S. Brattke, B.T.H. Varcoe, and H. Walther, Phys. Rev. Lett. **86**, 3534 (2001).
[15] Q.A. Turchette, Phys. Rev. Lett. **75**, 4710 (1995); A. Rauschenbeutel, G. Nogues, S. Osnaghi, P. Brune, J.M. Raimond, and S. Haroche, *ibid.* **83**, 5166 (1999).
[16] J.I. Sanchez-Mondragon, N.B. Narozhny, and J.H. Eberly, Phys. Rev. Lett. **51**, 550 (1983); Y. Kaluzny, P. Goy, M. Gross, J.N. Raimond, and S. Haroche, *ibid.* **51**, 1175 (1983); M.G. Raizen, R.J. Thompson, R.J. Brecha, H.J. Kimble, and H.J. Carmichael, *ibid.* **63**, 240 (1989); Y. Zhu, D.J. Gauthier, S.E. Morin, Q. Wu, H.J. Carmichael, and T.W. Mossberg, *ibid.* **64**, 2499 (1990).
[17] H.J. Carmichael, P. Kochan, and B.C. Sanders, Phys. Rev. Lett. **77**, 631 (1996); B.C. Sanders, H.J. Carmichael, and B.F. Wielinga, Phys. Rev. A **55**, 1358 (1997); L. Horvath, B.C. Sanders, and B.F. Wielinga, J. Opt. B: Quantum Semiclassical Opt. **1**, 446 (1999).
[18] See, e.g., A.S. Davydov, *Quantum Mechanics* (Pergamon Press, Oxford, 1965), p. 116.
[19] S.M. Tan, J. Opt. B: Quantum Semiclassical Opt. **1**, 424 (1999).
[20] C. Cohen-Tannoudji and S. Reynaud, J. Phys. B **10**, 345 (1977); C. Cohen-Tannoudji, J. Dupont-Roc, and G. Grynberg, *Atom-Photon Interactions* (Wiley, New York, 1992).
[21] H.S. Freedhoff and Z. Ficek, Phys. Rev. A **55**, 1234 (1997); A.D. Greentree, C. Wei, S.A. Holmstrom, J.P.D. Martin, N.B. Manson, K.R. Catchpole, and C. Savage, J. Opt. B: Quantum Semiclassical Opt. **1**, 240 (1999).
[22] A. Böhm, *Quantum Mechanics* (Springer, Berlin, 1979).
[23] S. Brattke, B-G. Englert, B.T.H. Varcoe, and H. Walther, J. Mod. Opt. **47**, 2857 (2000).